Earthquakes and Structures, *Vol. 12, No. 2 (2017) 251-262*
DOI: https://doi.org/10.12989/eas.2017.12.2.251

Seismic evaluation of soil-foundation-structure interaction: Direct and Cone model

Jahangir Khazaei*, Azadeh Amiri[a] and Mehrdad Khalilpour[b]

Faculty of Engineering and Technology, Razi University, Kermanshah, Iran

(Received September 11, 2016, Revised January 18, 2017, Accepted January 19, 2017)

Abstract. The present research intends to study the effects of the seismic soil-foundation-structure interaction (SFSI) on the dynamic response of various buildings. Two methods including direct and Cone model were studied through 3D finite element method using ABAQUS software. Cone model as an approximate method to consider the SFSI phenomenon was developed and evaluated for both high and low rise buildings. Effect of soil nonlinearity, foundation rigidity and embedment as well as friction coefficient between soil-foundation interfaces during seismic excitation are investigated. Validity and performance of both approaches are evaluated as reference graphs for Cone model and infinite boundary condition, soil nonlinearity and amplification factor for direct method. A series of calculations by DeepSoil for inverse earthquake record modification was conducted. A comparison of the two methods was carried out by root-mean-square-deviation (RMSD) tool for maximum lateral displacement and story shear forces which verifies that Cone model results have good agreement with direct method. It was concluded that Cone method is a convenient, fast and rather accurate method as an approximate way to count for soil media.

Keywords: soil-foundation-structure interaction; finite element method; Cone model; seismic excitation; infinite boundary condition

1. Introduction

Normally Earthquake is a natural disaster that can have devastating effects on structures in seismic regions and cause economic damage and casualties. Behavior of structures placed on rock differs from those built on soil. So, during the earthquake, structural response is affected by the interaction between structure, foundation and the supporting soil with dynamic filtering effects, which is named as soil-foundation-structure interaction (SFSI) phenomenon that plays an important role in dynamic analysis.

It is emphasized that the numerical methods are most appropriate and accurate methods for soil structure interaction (SSI) analysis (Chopra and Gutierrez 1974). Additionally, some remarkable considerations regarding the DSFSI phenomenon are developed by taking into account the experimental results, as well as comparing them with the numerical ones (Abate *et al*. 2010, Deng and Kutter 2012, Liu *et al*. 2012, Trombetta *et al*. 2013). Numerical formulations for SFSI systems are different. In addition, the finite deformation pattern in the finite element method (FEM) has also been well developed and some interesting results have been published in the literature (Huang *et al*. 2015). Two and three dimensional finite element analyses (FEAs) are able to fully incorporate nonlinear dynamic modeling of SFSI system where soil, foundation and structure are modeled as a whole system (Elgamal *et al*. 2008, Koutsourelakis *et al*. 2002, Zhang *et al*. 2003).

Due to the different point of view between geotechnical and structural engineering, geotechnical engineers usually pay more attention to the soil properties than the structures. On the other hand, structural engineers usually focus more on the structural properties. Accordingly, in simulating the soil–structure interaction phenomenon, sophisticated models are usually applied only to one aspect and the other aspect is rather compromised. Therefore, in order to increase the accuracy of numerical analysis for SFSI problems to such a level that satisfies requirements of both geotechnical and structural engineers, Bao *et al*. (2012) suggested a numerical method in which the soils and the structures are properly modeled (Bao *et al*. 2012). It has been implied that the role of the SFSI is usually considered beneficial to the structural system under seismic loading because it extends the period of the structure and increases the damping of the structural system (Hokmabadi *et al*. 2014). Matinmanesh and Asheghabadi concluded that all soil types amplify bedrock motions in the soil-structure interface and with different intensities. Many factors affect amplification including the soil type and properties, earthquake frequency content and the properties of the overlying building (Matinmanesh and Asheghabadi 2011). Recently, several researchers such as Sharma *et al*. (2014), Yeganeh *et al*. (2015), Ghandil and Behnamfar (2015, 2016) and etc. carried out studies for SFSI analysis for buildings with different heights supported by the raft and shallow foundation system by considering the 3-D and the 2-D

*Corresponding author, Assistant Professor
E-mail: j.khazaie@razi.ac.ir
[a]MSc
E-mail: azadeamiri44@yahoo.com
[b]Ph.D. Student
E-mail: mehrdad1189@yahoo.com

http://www.techno-press.com/journals/eas&subpage=7
ISSN: 2092-7614 (Print), 2092-7622 (Online)

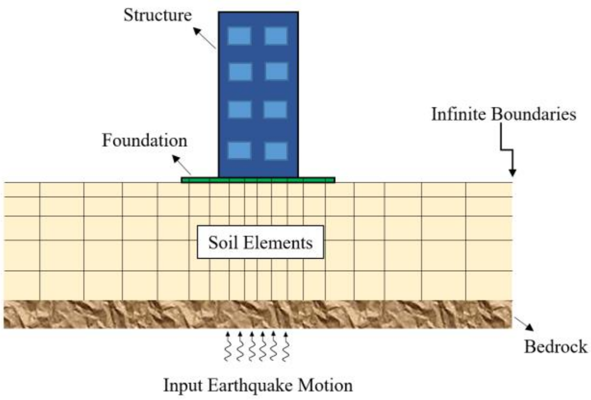

Fig. 1 Components of a Soil-Foundation-Structure System in direct approach

nonlinear analysis and confirmed the validity of numerical calculations with the expected results (Behnamfar and Banizadeh 2016, Ghandil and Behnamfar 2015, Han 2002, Isbiliroglu *et al*. 2014, Sharma *et al*. 2014, Yeganeh *et al*. 2015).

Numerical analysis methods of (SFSI) problems can be classified as direct and substructure approaches. In the direct method for analysis of SFSI it is necessary to model underlying soil, foundation and structure with best precision and accuracy since they are supposed to be analyzed together, Fig. 1.

Structure and foundation, as bounded medium can be modeled with any level of substantial details, but the main point is modeling the infinite dimensions of soil medium that can't simply be modeled with the finite elements. Several researchers developed a method that has proved to be very successful in dealing with infinite domains by introducing 'infinite' elements (Astley and Coyette 2001, Astley and Hamilton 2006, Bettess 1992).

In reality most geotechnical problems specially SFSI phenomena are three dimensional. This implies that three components of displacement must be accounted for and that the full three dimensional geometry must be considered in finite element analysis. FEM can simulate the mechanics of soil and structures better than other methods, deal with complicated geometry and applied load, and determine non-linear phenomena. To this date, there are many general-purpose programs developed by commercial corporations for research in the engineering field (Lou *et al*. 2011). In substructure method, soil-structure system is divided into two parts: first part is structure and the second part is the soil that has common boundary with foundation and each part can be modeled in detail (Wolf 1985).

Various formulations do exist in substructure method. Three different types of models are available: lumped-parameter models, consisting of a few degrees of freedom connected by springs, dashpots and masses with constant frequency-independent coefficients; representations based on prescribed wave patterns in the horizontal plane of one-dimensional body and surface waves and cylindrical waves; and cone models (Wolf and Deeks 2004). Among mentioned methods, Cone model is based on a rather strong and innovative theory and is so much easier to use. In this method the unbound soil medium is to be simulated by springs and dashpots for all degrees of freedom. Cone models provide sufficient accuracy for practical engineering designs. Considering the vast uncertainties in determining the dynamic properties of the soil, this deviation can be accepted for practical engineering problems (Mohasseb and Abdollahi 2009).

So evaluating the validity and performance of the Cone model, and comparison with the direct method are the main objectives of the present paper. To attain this goal, response of various 3D FEM examples are investigated. The accuracy of the dynamic response of buildings using cone models for the soil has been studied in detail studied.

2. Cone model approach for SFSI system

Cone model is based on one-dimensional strength of materials theory; an approximate method that considers the soil medium with conical bars and beams. According to the assumptions of this method a one-dimensional model propagates the seismic wave over a traveling path in a conical bar by conveying a wave through its cross section, Fig. 2(a). The incident wave propagates away from the disturbance area by widening its cross section as it travels on, while the travel path of the wave remains perpendicular to horizon at each depth (Wolf and Deeks 2004).

In a layered half space medium, a lot of reflected and refracted waves propagating in their own cones at the discontinuity of the material properties corresponding to an interface of the soil layers is encountered, Fig. 2(b). As it is illustrated A continuous follow up procedure of each incident wave and superposing them leads to a resultant wave pattern.

Generally, cone models are divided into two categories: translational and rotational. So, the vertical, horizontal, rocking and torsional dynamic stiffness of a soil layer or a half-space can be captured using cone concepts.

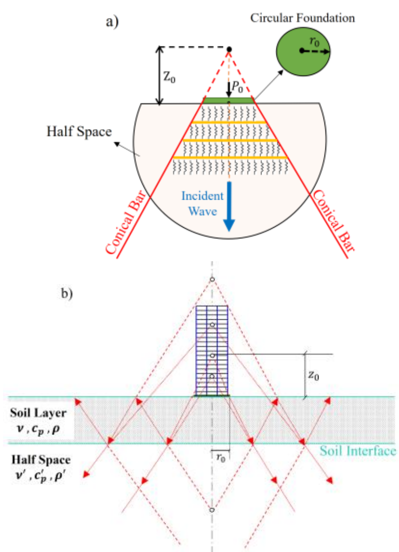

Fig. 2 (a) Cone model theory (b) reflected and refracted waves at a material discontinuity propagating in their own cones

3. Numerical modeling

3.1 Steel frame structure modeling

Two steel moment resisting frame (SMRF) structures with total heights of 15 m (5-story) and 60 m (20-story), representing conventional types of short and tall buildings, were selected for this study. The sections used in the design are displayed in Table 1. The columns are considered to have a fixed connection to the foundation. The columns are spliced above the 5th and 10th floor. All columns and girders are designed as Box and I shaped sections respectively.

Floors are concrete slabs with 0.3 m thickness. Both buildings are placed on rectangular mat footings. The connection between the foundation and the bottom of first story column is modeled as the rigid connections. The characteristics of the buildings were obtained from the preliminary design of the buildings following the routine design process according to the AISC (Merritt 1996).

Material properties of the buildings and foundation are presented in Table 2. An isotropic plastic hardening was considered for steel members. In this table ρ, E and ν are mass density, modulus of elasticity and Poisson ratio respectively. Both rigid and flexible foundations are considered. It should be noted that in order to use the Cone model for SFSI problems, rectangular foundation should be transformed into an equivalent circular one. For example the 24×18 m foundation of the 20-story building has an equivalent radius about 11.73 m, Fig. 3.

Table 1 Typical sections of 5 and 20-story buildings (for I section girders, 2×flange×thickness+web×thickness)

No. Stories	Elevation (m)	Girders (mm)		Column (mm)
		x-direction	*y*-direction	
5-story	0-15	2×220×15+340×15	2×220×15+340×15	Box 420×40
20-story	0-15	2×300×15+420×15	2×260×15+380×15	Box 520×40
	15-30	2×260×15+380×15	2×240×15+360×15	Box 480×40
	30-60	2×240×15+360×15	2×220×15+340×15	Box 420×40

Table 2 Material Properties of the buildings and foundation

	Material	Mass Density (kg/m^3)	Elastic		plastic	
			E (*pa*)	ν	Yield Stress (*pa*)	Plastic strain
Structures	Steel Frame	7850	2.10E11	0.3	3.416E8	0
					4.307E8	0.05
					5.099E8	0.14
					4.947E8	0.2
Foundation	Concrete Slab	2550	1.22E12	0.2	-	-
	Concrete	2400	2.1E9	0.2	-	-

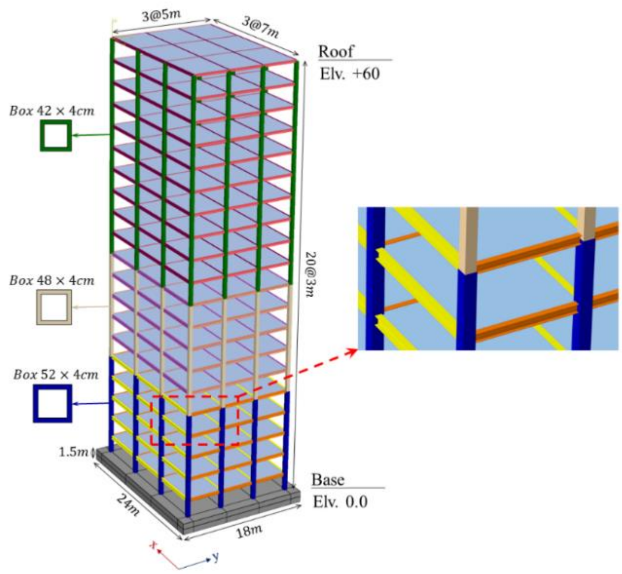

Fig. 3 Geometrical details of 20-story structure and foundation

Table 3 The Mechanical properties of soil

Layer	Thickness (m)	$E(kPa)$	$\rho(\frac{kg}{m^3})$	ϑ	$C(Pa)$	$\emptyset^{\circ}$	$C_s(\frac{m}{s})$	$\Psi^{\circ *}$	$\zeta(\%)^{**}$
1	15	131.888e3	1936.8	0.33	10000	30	160	2	5
2	10	189.883e3	2038.7	0.29	20000	34	190	4	5
3	5	289.467e3	2242.6	0.22	25000	37	241	7	5

*dilatancy angle; **damping ratio

3.2 Soil model

The site is accommodated in a high seismicity region on the D-type as a stiff sandy soil, according to AISC code. In this study an elastic-perfectly plastic behavior was considered for the soil medium using Mohr-Coulomb yield criterion with unassociated flow rule. During the cycles of design and analysis the dimensions of the bulb below and around the structures where the soil response is different from the free-field response was investigated. Also the reason for choosing a soil deposit thickness of 30 m for numerical models is that In most cases the amplification mainly occurs within the first 30 m of the soil profile, which is in agreement with most modern seismic codes calculating local site effects based on the properties of the top 30 m of the soil profile (Rayhani and El Naggar 2008). Optimum width of the soil medium is calculated from various trials. Therefore, Soil medium has 200*200*30 m for the SSI analysis. According to the Table 3, the engineering properties of the soil medium has been explained in details where E is Elastic modulus, C is cohesion stress, ϕ is friction coefficient, C_s is shear wave velocity, Ψ is dilatancy and ξ is damping ratio (Duggal 2000).

4. Dynamic analysis

4.1 Earthquake record selection and modification

Three seismic records of Northridge, Duzce and Tabas, each containing consistent accelerograms, are selected from the PEER Strong Motion Database according to ASCE7-10. The selection criteria for ensuring consistency of the records are magnitudes, fault type, distance and source mechanisms as mentioned in Table 4.

For three-dimensional analyses, ground-motions should have at least a pair of appropriate horizontal ground-motion acceleration components. Scaling of the ground motions has been done based on ASCE7-10 for each independent earthquake, such that for each pair of horizontal ground-motion components, a square root of sum of the squares (SRSS) spectrum was conducted by taking the SRSS of the 5% damped response spectra of the unscaled components.

Each pairs of motion are then scaled with the same scale factor such that the mean of the SRSS spectra from all horizontal component pairs does not fall below the corresponding ordinate of the target spectrum in the period range from $0.2T_n$ to $1.5T_n$, where T_n is the fundamental period of each structure, Fig. 4. This figure shows the spectral accelerations of the soil records before and after scaling for the 20 story building with T=2.51 s. The limits on the number of ground motions according to ASCE/SEI 7 is based on engineering experience instead of a comprehensive evaluation (Reyes and Kalkan 2011).

Table 4 Utilized earthquake motions and their scaled factors

Event	Year	Fault	Type	Magnitude	Joyner-Boore Distance (R_{jb})	Soil type	Scale Factor 20 story	Scale Factor 5 story
Tabas (Iran)	1978	reverse	far field	7.35	25	D	2.8	1.6
Northridge (USA)	1994	reverse	far field	6.69	28	D	1.9	1.2
Duzce (Turkey)	1999	reverse	far field	7.14	30	D	1.7	0.97

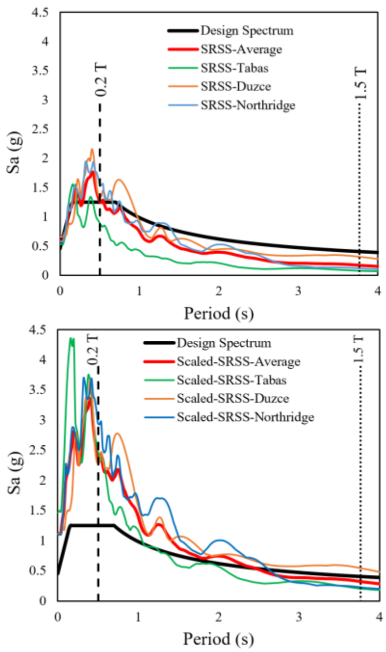

Fig. 4 Response spectrum before and after scaling the earthquake records for 20 story building

4.2 Free field response analysis

In order to determine the signal at bedrock, it is necessary to solve an inverse wave propagation problem and reconstruct the acceleration time history at the bedrock from a given recorded signal at the top of free surface (Feldgun *et al*. 2016). Accordingly, the 1D dynamic analysis of the inverse wave propagation of the free field site is implemented for Tabas record with DeepSoil software. The shear modulus and damping ratio decay curves suggested by Seed and Idriss (1991) (Mean Limit) are assumed and implemented for soil layers, Fig. 5.

The corresponding bedrock motion is then calculated and provided as shown in Fig. 6. Then both computed components of bedrock accelerations are employed in an ABAQUS free field model simultaneously. Fig. 7 compares the resultant acceleration component of Tabas surface X-direction with ABAQUS free field. Despite the different solving equations in DeepSoil 1D and a 3D model in ABAQUS a good agreement is observed.

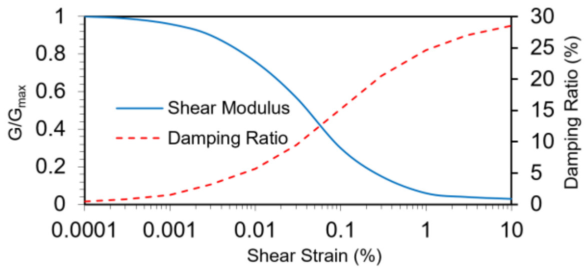

Fig. 5 G/G_{max} and damping ratio (%) are defined as functions of shear strain (%)

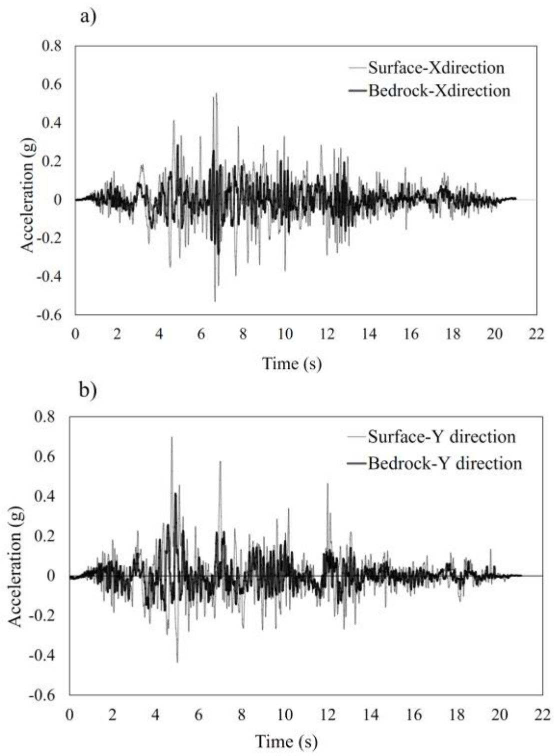

Fig. 6 Bedrock record and soil surface record under the influence of Tabas earthquake for (a) X and (b) Y directions

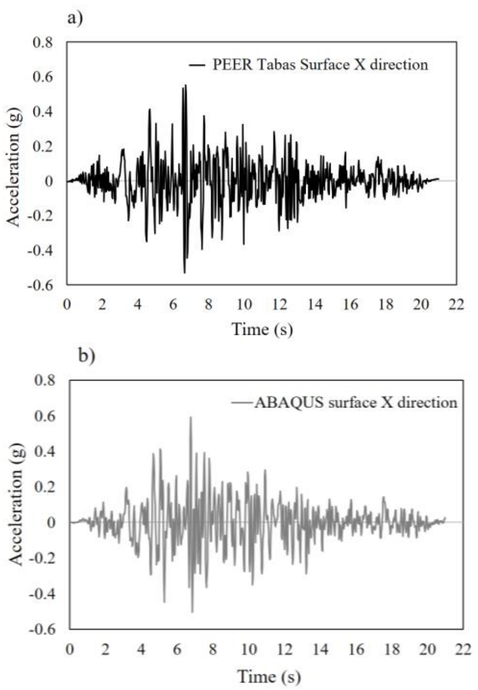

Fig. 7 Acceleration component of Tabas surface X-direction (PEER) Vs. ABAQUS free field results at surface

4.3 Infinite Boundary condition

In present study, infinite boundary condition has been modeled in order to avoid the multiple reflections during the dynamic analysis. Infinite elements are represented to simulate the far field soil to account for the energy absorbed from the unbounded soil domain while horizontal deformation was also simulated realistically. The three-dimensional, 8-node linear one-way infinite brick (CIN3D8) elements were used (Zienkiewicz *et al*. 1983).

The infinite elements maintain the static stresses achieved at the end of the static (gravity) analysis step, so there is no need to displace the boundaries for the time-history dynamic analysis. Boundary damping constants were chosen to minimize the reflection of normal and shear wave energy back into the finite element mesh as

$$d_p = G\frac{\lambda+2G}{c_p};\ \ d_s = \rho c_s \tag{1}$$

Where d_p and d_s are the distributed damping of the boundary in the normal and shear directions, respectively. The dynamic response of the infinite elements is as plane body waves that travel to the boundaries orthogonally. The governing equation of motion in the boundaries is as

$$\rho\ddot{u}_i = G\frac{\partial^2 u_i}{\partial x_i \partial x_j} + (\lambda + G)\frac{\partial^2 u_j}{\partial x_i \partial x_j} \tag{2}$$

Where ρ, G, λ are soil properties, c_p and c_s are the velocities of the normal wave and shear wave respectively, u_j is the material particle displacement, x_i and x_j are the positions of noted i and j.

So the soil will be modeled with the lowest number of elements and degrees of freedom. A good way to measure

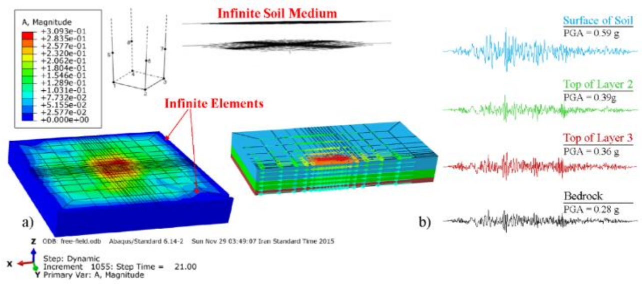

Fig. 8 (a) Infinite medium of the soil and accurate performance of infinite boundaries) b) amplified earthquake records

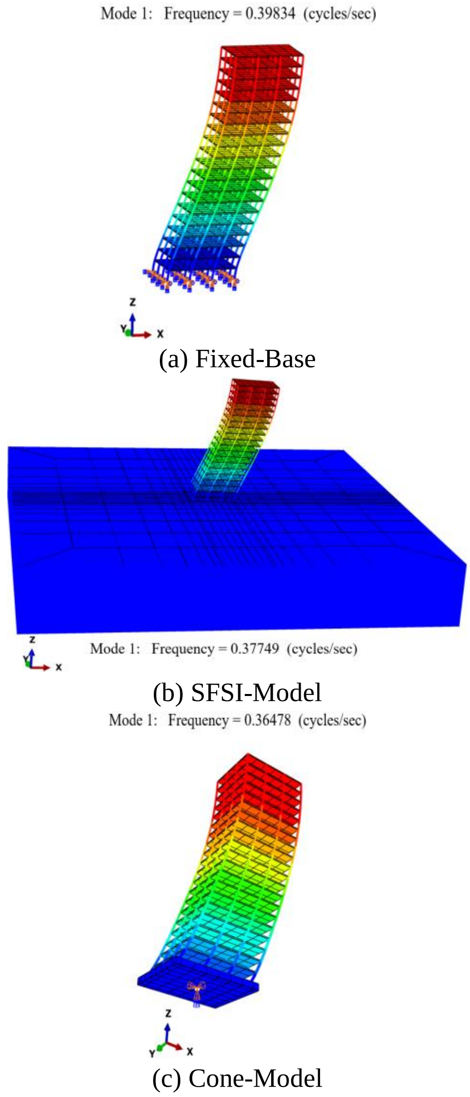

Fig. 9 Eigenvalue Results for 3 modes in (a) fixed base, (b) SFSI and (c) cone model

the ability of the infinite boundary to absorb impinging elastic waves is free field analysis of the soil as mentioned in section 4.2. Dynamic response of infinite element is based on considering the vertical motion of plane waves toward the boundaries. Fig. 8 demonstrates the propagation of acceleration contours with maximum amount in the mid surface of the soil and zero for infinite boundary elements which clearly verifies the accurate performance of infinite boundaries under Tabas earthquake.

4.4. Modal analysis

The modal analysis was performed to determine natural modes of frequencies for the soil and structural model. The results of modal analysis are used for dynamic analysis. Modal analysis are performed to determine the Rayleigh damping coefficients and vibrational frequency of the SFSI system. For that Lanczos Eigensolver (Hibbitt 2013) all frequency ranges is implemented. A results of first mode Eigenvalue analysis for SFSI, fixed base and cone model for the previously mentioned 20-story building are shown as period values in Fig. 9. Rayleigh damping is a very common and efficient type of damping implementation used in the incremental finite element analysis (Manolis and Markou 2012).

The standard damping matrix equation is

$$[C] = \alpha[M] + \beta[K] \tag{3}$$

Where α and β are coefficients of mass and stiffness matrices where ω_1 and ω_2 are two different and dominant circular frequencies respectively

$$\alpha = \frac{2\zeta\omega_1\omega_2}{\omega_1+\omega_2} \qquad \beta = \frac{2\zeta}{\omega_1+\omega_2} \tag{4}$$

4.5 CONAN program and verification

As mentioned in section 2 Cone model has a rather complex procedure in SFSI problem. To calculate the dynamic soil stiffness a MATLAB Program can be used. For this, CONAN software which is a MATLAB written program is employed to carry out the calculation of spring and damper coefficients. First, Soil characteristics, including shear modulus, layering, Poisson's ratio, mass density, material damping ratio and the equivalent radius of the circular foundation needs to be defined in a text file, then this file is called by the CONAN software, and for all degrees of freedom spring and damper coefficients are obtained individually for the surface and embedded foundations Table 5.

To gain confidence in employing cone models, a methodical evaluation of the accuracy for layered half-spaces is essential. To assess the accuracy of the dynamic stiffness coefficients from CONAN program, surface and embedded foundations for all degrees of freedom have been compared with exact solution as proposed by (Wolf and Deeks 2004). For example, as it is observed in Fig. 10 the deviations for the 20-story with surface foundation SFSI system are almost smaller than typical engineering accuracy of ±20% curves. This criterion is specifically suggested by (Wolf and Deeks 2004) for Cone model approach accuracy evaluation.

4.6 Analysis procedure

All models are analyzed for both static and then seismic loading conditions. The system is modeled initially for gravitational static loading to get the initial stress condition which includes the self-weight of structure, foundation and

Table 5 Coefficients of springs and dashpots from CONAN program

		20 Story building		5 Story building	
Horizontal	K	3.5264E+9	4.4757 E+9	1.7617 E+9	2.0457 E+9
	C	5.2652 E+8	6.6737 E+8	1.7351 E+9	2.3030 E+9
Vertical	K	5.7626 E+9	6.4034 E+9	4.8166 E+9	6.3273 E+9
	C	1.5814 E+8	9.1150 E+8	1.6033 E+9	1.9483 E+9
Rocking	K	4.3880 E+11	5.4737 E+11	2.9738 E+11	4.7547 E+11
	C	4.4836 E+10	5.7266 E+10	4.9233 E+10	8.4185 E+10
Torsional	K	5.4394 E+11	7.4556 E+11	3.6346 E+11	7.0611 E+10
	C	5.5075 E+10	7.5564 E+10	5.9674 E+11	1.4398 E+11

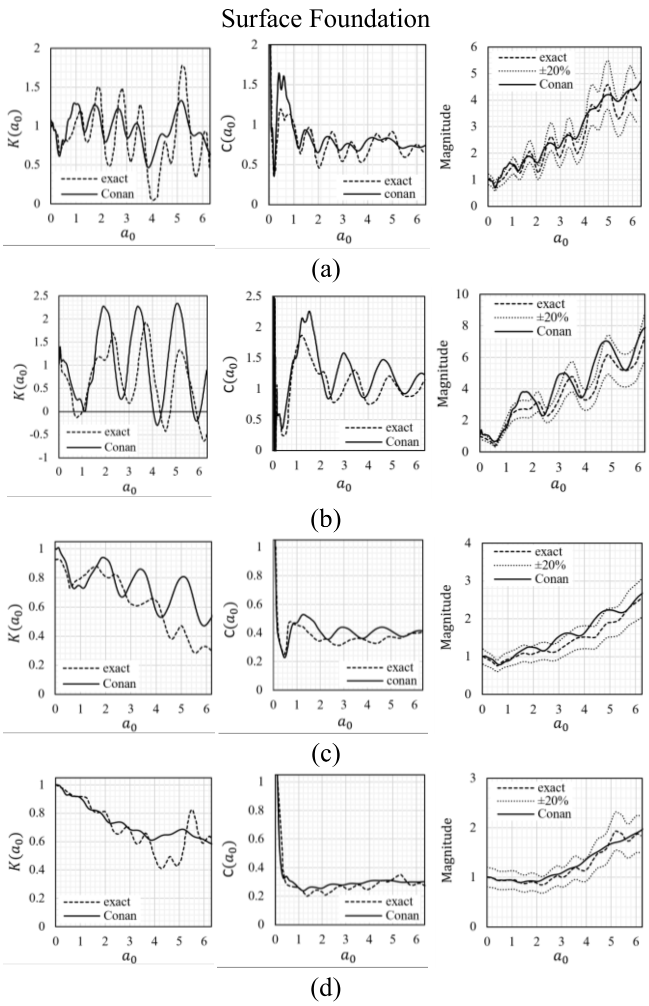

Fig. 10 Dynamic-stiffness coefficients of surface disk on three layers fixed at base. a) Horizontal. b) Vertical. c) Rocking. d) Torsional

soil system for the dynamic analysis. Once the static analysis has been completed the dynamic analysis starts. Attained acceleration from sec 4.2 is now applied to the bed rock. The stresses and displacement so obtained at the end of static analysis has been considered as the initial response for the dynamic analysis. Three main category including fixed-base, Cone and SFSI models are being discussed in this paper. In fixed-base model, the structure is being analyzed without soil and foundation with fixed boundary condition to resist all displacements or rotations at the bottom. In Cone model the structure is built on a rigid foundation with springs and dashpots in the bottom in place of soil. The SFSI models include whole environment of soil, foundation and structure as direct method approach.

The first step in FEM analysis considering SFSI is extent determination of the soil media to be considered for the analysis. As already discussed, in SFSI analysis using FEM, the infinite soil medium is reduced to a finite region using infinite element boundaries. It is noteworthy to state that the optimum width of the soil medium is arrived from various trials. A too coarse mesh may deviate from the expected response, whereas a too fine mesh requires very long computational time. Therefore, a tradeoff is required to obtain an approximately accurate solution in reasonable time. Hence, some trials in order to capture the optimum mesh size for soil medium was carried out. Then, as it is seen in Fig. 11 a mesh pattern for the SFSI system with large elements at lateral soil boundary and fine elements near the building is considered. Soil is modeled using 8-node solid 3D Stress brick elements whereas shell and beam elements with proper material orientations were applied to story floors and frames, respectively. Overall 18470 elements for 20 story SFSI model and 8132 for 5 story SFSI model is used.

To investigate the optimum interaction between different mediums an effort was made to converge and overlap mesh nodes at the end of columns to the foundation and in turn the foundation interface to the soil. The interface between the foundation and soil has been modeled as a surface to the surface contact. Since the tangential and normal behavior of the contact surfaces can influence the results of the numerical simulation, mechanical properties of the contact surfaces should be chosen with great rigor.

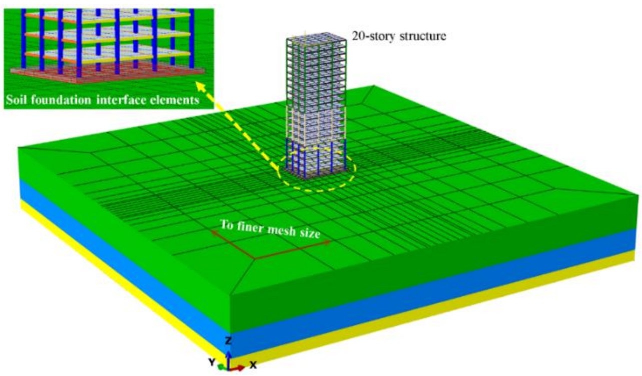

Fig. 11 Mesh pattern for the soil-foundation-structure system with infinite boundary condition and soil-foundation interface elements

Table 6 Type of Interface Interaction

Friction coefficient (μ)	0	0.176	0.268	0.364	0.466	0.577
Internal	Frictionless	$\frac{1}{3}\varphi$	$\frac{1}{2}\varphi$	$\frac{2}{3}\varphi$	$\frac{5}{6}\varphi$	φ

In order to model the tangential behavior of soil-foundation contact surfaces in the finite element model, a subroutine is developed in the FORTRAN programming language and linked to ABAQUS. This subroutine should be capable of reserving the required variable in a way that corresponds to the classical Mohr-Coulomb failure model. Since the Mohr-Coulomb failure model cannot be directly employed in the ABAQUS, to define the isotropic frictional coefficient between the contacting surfaces, a modified version of this model was coded in the FRIC_COEF subroutine according to

$$\mu = \tau/\sigma = \tan(\varphi) + \frac{c}{\sigma} \tag{5}$$

Where μ is the coefficient of friction, τ is the shear strength, σ is the normal stress, c is the cohesion intercept of the failure envelope, and φ is the slope of the failure envelope or the internal friction angle. In this study a surface to surface tangent and tie interaction elements are used, Table 6.

5. Results and discussion

5.1 Effects of friction coefficient

One of the important parameter governing the design of SFSI system is the friction coefficient of sliding surface. The response of the structure varies with friction coefficient. It is well known that sliding displacement decreases with increase in friction coefficient and the optimum friction coefficient at which base shear is minimum can be found (Krishnamoorthy and Anita 2016). It is observed that for 20-story building the SFSI has small effect on displacement response of the structure on this D type soil profile for the range of friction coefficient considered in this study. The sliding displacement of the structure decreases with increase in friction coefficient. However, the SFSI effect on sliding displacement of the 20-story structure is influenced by friction coefficient in a way that the SFSI effect is large at small values of friction coefficient and the effect decreases with increase in friction coefficient. As observed for the implied far field Tabas earthquake SFSI is rather detrimental at low friction coefficient and show advantageous effect at large value of friction coefficient, Fig. 12(a).

Base shear of the 20-story structure on linear and nonlinear types of soil with deformable foundation initially reaches a maximum value and then decreases with further increase in friction coefficient whereas for linear and nonlinear types of soil with rigid foundation a decreasing trend for all friction coefficient range can be observed. For structures with rigid foundations on either nonlinear or linear soils, the SFSI effect is large and detrimental at

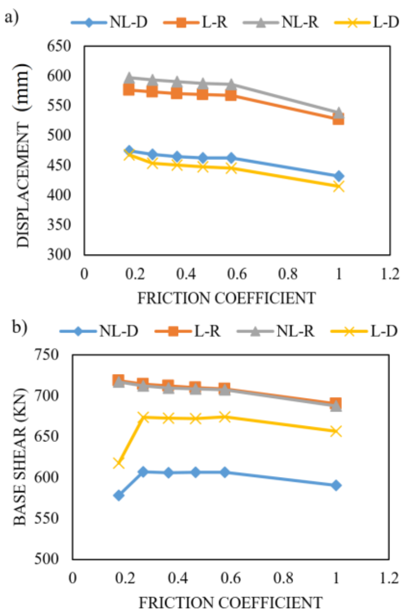

Fig. 12 Variation of response of 20-story structure with friction coefficient

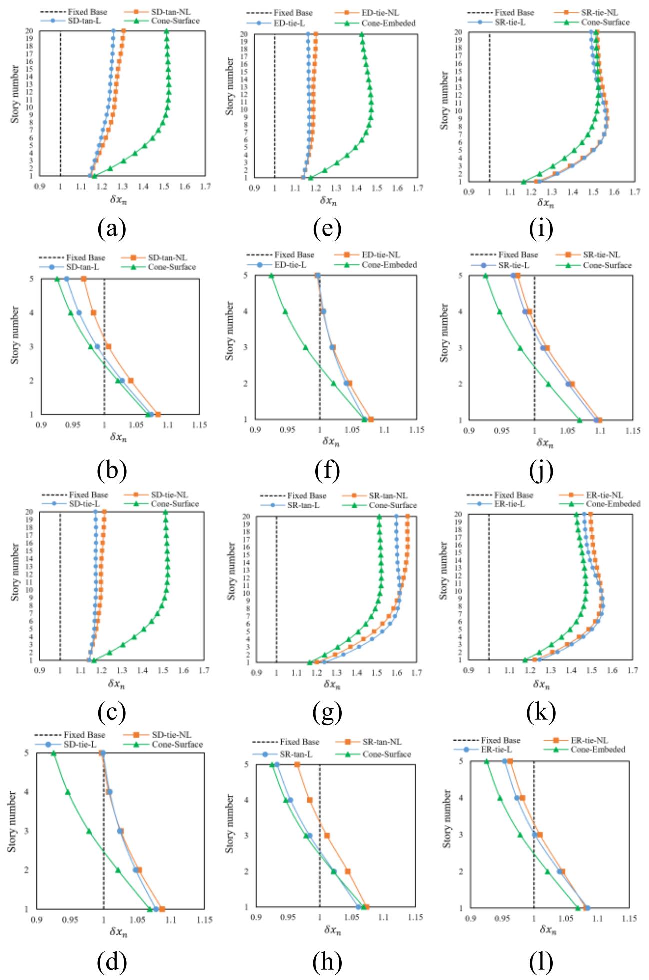

Fig. 13 Normalized displacement variation in Linear and Nonlinear SFSI cases and comparison with Cone

small values of friction coefficient, this effect decreases with increase in friction coefficient and SFSI effect reaches a minimum value near optimum friction coefficient, and, SFSI starts showing beneficial effect for higher values of friction coefficient increases, Fig. 12(b). That is at high value of friction coefficient or tie interaction, the structure is in non-sliding phase at all time during earthquake that for all models a beneficial SFSI consideration is observed. This is an interesting observation in the sense that near the optimum friction coefficient SFSI has small effect on both the base shear and sliding displacement response of the structure. In the case of far field Tabas earthquake for which the optimum friction coefficient is small, the SFSI effect is beneficial at almost all the friction coefficient.

5.2 Lateral displacement

Results of 3D numerical predictions for the maximum lateral displacements of the fixed base, Cone and direct model are summarized and compared in Figs. 13-15 for 20 and 5 story buildings which represent high rise and low rise buildings. A plot of maximum deformation along X-axis versus story height shows higher value for the SFSI and Cone model than the fixed base model. Maximum responses with SFSI under Tabas earthquake is called $x_{n(SFSI)}$ for nth-story. These are then normalized to the corresponding values of models with no SFSI (x_n) consideration. In the following figures $\delta x_n = x_{n(SFSI)}/x_n$. It is observed that in spite of the 5-story building responses, lateral displacement of stories is increased due to SFSI with respect to the Fixed-Base case. The observed disparity between direct method prediction and Cone model can be due to the nature of numerical methods, the models employed to simulate the complicated dynamic behavior of the soil, the assumption of an ideal connection between the structural elements, and unavoidable numerical uncertainties.

5.2.1 Effect of soil nonlinearity

In most cases, the NL modeling of soil has resulted in more lateral displacements of stories that is something intuitively predictable. Fig. 13 Shows the difference between structure displacement for linear and nonlinear soil. In 20-story building the total displacement of the system tends to increase as the height of the structure increases. However, on the contrary, for the 5 story building rotation of the assumed foundation cannot increase the lateral displacement significantly and the response decreases or increases slightly based on the story level and applied soil model. a comparison for both model structures indicates that the increase in the maximum lateral displacement was more severe for the 20-story model structure in comparison with the 5-story model structure. This is because of the fact that the rocking component results in more lateral displacement as the height of the structure increases. For deformable foundation in the 20-story building with linear soil behavior, less displacement comparing nonlinear soil is observed, Figs. 13(a), (c), (e). While for rigid foundations when linear and nonlinear behavior of soil is taken into account the structural displacement varies for different stories, some equal, less or higher, Figs. 13. (k), (i), (g). On the other hand, for almost every model in the linear soil less displacement in compression with nonlinear soil is noted except for Figs. 13(d)-(f) which has equivalent top story displacement for both soil models. Generally, nonlinear modeling of soil results in increased lateral displacements of stories that is something intuitively predictable.

Maximum difference between Cone model with respect to the surface deformable foundation models with tangent interaction and linear and nonlinear soil is 28% and 25%, while for tie interaction with linear and nonlinear soil these values are 29% and 34% respectively Figs. 13(a)-(c). This difference is approximately 29% for embedded deformable foundation model Fig. 13(e). Five-story building displacement Cone model trend shows best agreement with SD-tan-L with about 4% and the most difference is observed in SD-tie-L with around 8% Figs. 13(b), (d), (f).

It is noticed that for 20-story building with rigid foundation and specifically with tie interaction is in good agreement with Cone model and SFSI models Figs. 13(g), (i), (k) though, for 5-story building this was seen in tangent interaction and linear soil Figs. 13(h), (j), (l).

5.2.2 Effect of rigid and deformable foundation

Fig. 14 shows the displacement difference between Cone model and rigid or deformable foundations. Also as observed from Figs. 13-15 rigid assumption of the foundation causes a growing trend in comparison with the deformable foundation which doesn't seem to be beneficial to the analysis whereas displacement response of 5-story building with rigid and deformable foundation are almost equal. As mentioned above for 20-sory building unlike 5-sory building with any SFSI model story displacement grows as the building height increases. For 20-story building using rigid foundation ascends the structural displacement about 5-37 percent. However, for 5-story building this difference ranges from 0.04-1 percent. From Fig. 14 it could be clearly seen that Cone model is in best agreement with rigid foundation models for both 20 and 5 story buildings.

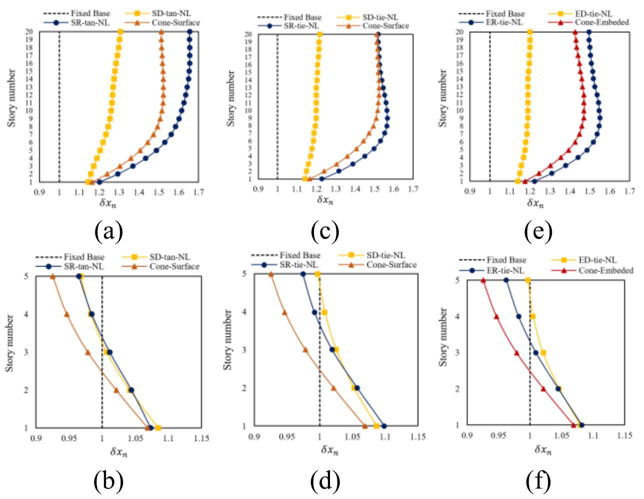

Fig. 14 Normalized displacement variation in Rigid and Deformable foundation SFSI cases and comparison with Cone model

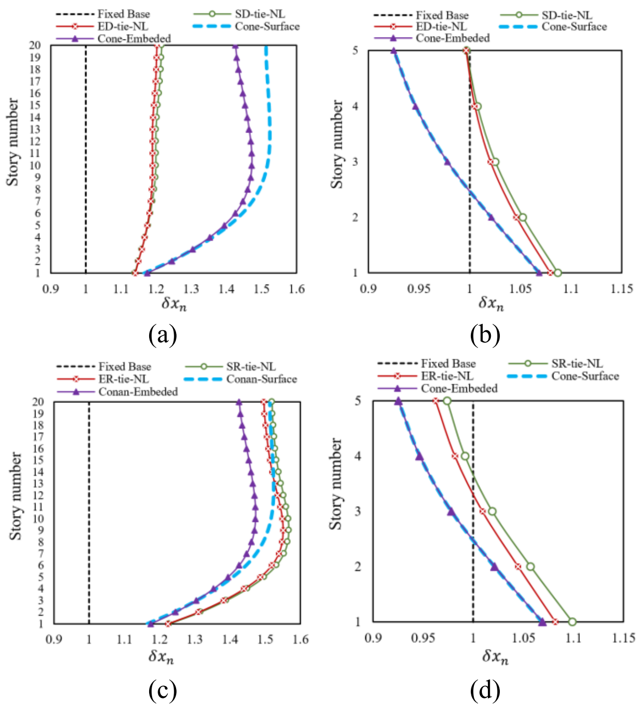

Fig. 15 Normalized displacement variation in Surface and Embedded foundation SFSI cases and comparison with Cone model

5.2.3 Effect of surface and embedded foundation

Fig. 15 shows different structural displacements of surface and embedded foundation for 20 and 5 story buildings. For 20-story building the observed difference is about 0.3-3% between surface and embedded Cone models and this deviation is growing for higher stories. Furthermore, a good agreement between for almost any model with rigid foundation and Cone models is noted Figs. 15(a)-(c). For 5-story Cone models with surface and embedded foundation cases a good tendency with negligible difference is seen. In these cases, deformable and rigid foundation have 0.32-1.5% and 0.28-2.5% variation respectively Figs. 15(b)-(d).

The root-mean-square deviation (RMSD) is calculated for each case to evaluate the accuracy of the modeling method. The RMSD is a frequently used technique to measure the difference between values predicted by a model and the values actually observed. The RMSD can be calculated as follow

$$RMSD = \sqrt{\frac{\sum_{i=1}^{n}\left(\frac{x_{ci} - x_{ai}}{x_{ci}}\right)^2}{n}} \tag{6}$$

Where x_{ci} is the maximum response by Cone model, x_{ai} is the maximum response of one another model and n is the number of stories.

The RMSD's for the maximum displacements of the buildings are calculated using Eq. 23. Table 7 shows the RMSD for various SFSI modeling techniques applied to the 5 and 20-story building and summarizes the RMSD values for these considered buildings. It is clear from this table that the cases selected above have been appropriate for SFSI analysis and ignoring SFSI in these cases result in considerable deviations. The largest deviation associated with overlooking SFSI belongs to the taller building (SD-tie-L) in Cone surface and (ED-tie-L) in Cone embedded model for 20story building. On the other hand, the SR-tie-NL for 20 story and SR-Tan-L for 5 story building are proved to be the most accurate one among the others in Cone surface and embedded models.

5.3 Distribution of story shear forces

The story shear seismic response of the structure as well as internal forces over the height of the structural elements is selected as response parameters as these are generally considered the most important parameters in seismic design practice.

The effect of SFSI on the story shear response profile for 5 and 20-story buildings is calculated using the two different analysis methods and compared to that obtained from fixed-base model. Story shear envelopes of the 20 and 5-story buildings are illustrated in Fig. 16. The envelopes show similar trends and make an evident fact that SFSI reduces the story shears. Inspecting the whole set of graphs shows that the reduction in story shear is larger for lower stories, taller buildings, and is negligible for upper stories of the taller buildings. In addition, the base shear, i.e. the story shear at the first story, obtained from the cone and direct model is from 45 to 55 % smaller than that of the fixed-base model. Values of the story shear RSMD's are presented in Table 8. The SR-tie-NL shows the maximum accuracy by 14.12% deviation. The deviation values ascend when SFSI is neglected and vary between 14-45 %.

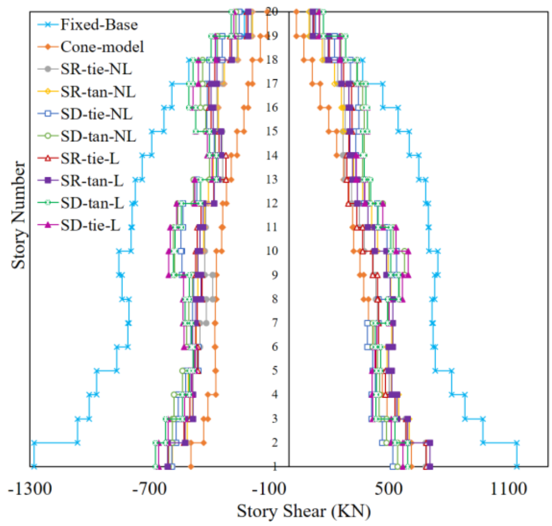

(a) 20-story building

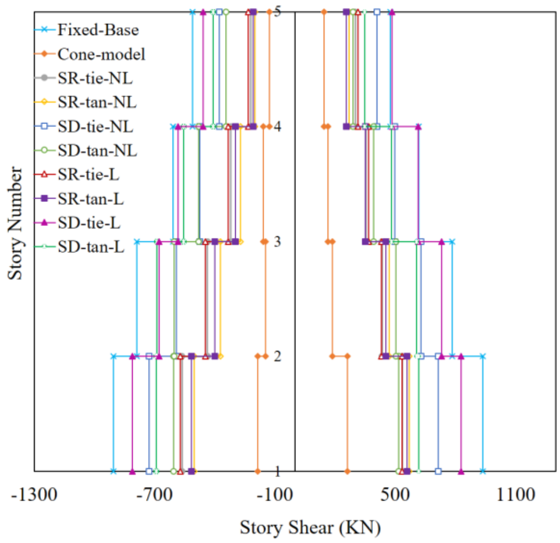

(b) 5-story building

Fig. 16 Story shear envelopes for 20 and 5 story buildings

Table 7 RMSD's for the maximum displacements of 5 and 20-story buildings

Name of Model	Type of Model	20-story building	5-story building
Cone-Surface	SD-tan-NL	14.58	3.18
	SD-tie-NL	18.47	5.24
	SR-tan-NL	7.23	3.18
	SR-tie-NL	4.00	4.21
	SD-tan-L	16.47	1.14
	SD-tie-L	19.99	5.21
	SR-tan-L	6.83	0.68
	SR-tie-L	4.31	3.57
	SD-rough	15.48	4.70
	SD-tan-0.19	15.57	4.76
	SD-tan-0.28	14.57	2.87
	SD-tan-0.38	14.30	1.82
	SD-tan-0.48	14.67	3.78
	Fixed Base	31.41	5.44
Cone-Embedded	ED-tie-NL	16.47	4.95
	ER-tie-NL	5.18	3.06

Table 8 RMSD's for the story shears of 20-story building

	Fixed Base	SR-tie-NL	SR-tan-NL	SD-tie-NL	SD-tan-NL	SR-tie-L	SR-tan-L	SD-tie-L	SD-tan-L
RMSD (%)	117.25	14.12	23.78	29.39	36.15	16.67	23.01	37.78	45.00

6. Conclusions

The study altogether provides useful guidelines for seismic design of buildings including the effect of soil. In this study, the effects of seismic SFSI is analyzed for typical 5 and 20-story building resting on raft foundation. The influences of parameters including Nonlinear/Linear soil assumption, Embedded/Surface and Deformable/Rigid foundation are investigated using two methods: direct method and Cone model. Structural responses are used to evaluate the effects of SFSI on the maximum story shear and displacement for the 5 and 20-story buildings.

Tabas bed rock earthquake record in two perpendicular directions has been implemented in direct method models and soil amplification due to the soil stiffness change is observed. In SFSI cases a verity of friction coefficients recommended by common codes between soil and foundation interface has been studied to find the optimum friction coefficient.

Cone model proposes semi-analytical equations for modifying properties of the linear soil by considering dominant structure frequencies, Poisson ratio and etc. Since the accuracy evaluation of Cone method was the main goal of this research, a verity of examples were considered to introduce steps of employing the Cone method and to investigate its accuracy and performance. The main findings of the study are summarized as follows:

- By considering lateral displacement and base shear factors a verity of friction coefficient as recommended by common code practice were investigated and it is concluded that an optimum friction coefficient for soil-foundation interface ranges from $\frac{1}{3}\phi$ to $\frac{2}{3}\phi$.
- Modal analysis results show that SFSI effect increases the period of the structure with respect to the fixed base cases and the increase of these values depend on soil type and structural stiffness. As the structural stiffness in comparison with soil or building height increases, the period rate increase as well. The same values that corresponds well enough to the SFSI models was observed for Cone model.
- Maximum lateral displacement of structures increases with the increasing number of stories so upper stories displacements are more affected with SFSI than the lower stories. However, 5-story building does not follow the same trend and lateral displacement changes for different floors. Cone models are in good agreement with the mentioned results.
- The story shear responses are highly dependent on the foundation and soil stiffness. By considering the SFSI, base shear for both 5 and 20 story building with respect to the fixed base model is decreased. Cone models are in good agreement with this trend as well.
- The story shear responses are highly dependent on the foundation and soil stiffness. By considering the SFSI, base shear for both 5 and 20 story building with respect to the fixed base model is decreased. Cone models are in good agreement with this trend as well.
- RMSD values compare all cases with Cone model based on lateral displacement and story shears. It was shown that almost in all of the cases the Cone method possesses a superior accuracy and concludes that the cone models results are promising.

Consequently, according to the obtained results from the comparison between approximate Cone models with SFSI model cases with a group of variables regarding soil and foundation that are used in this study, the high engineering efficiency of Cone model in order to consider soil-foundation-structure interaction is rather approved. Main features of Cone model method include reduced time of computation, acceptable engineering accuracy and accounting for all degrees of freedom including horizontal, vertical, rocking and torsional dynamic stiffness. Therefore, this method can be an alternative and convenient way for practical engineering designers to count for SFSI phenomena in seismic considerations.

References

Abate, G., Massimino, M., Maugeri, M. and Wood, D.M. (2010), "Numerical modelling of a shaking table test for soil-foundation-superstructure interaction by means of a soil constitutive model implemented in a FEM code", *Geotech. Geol. Eng.*, **28**(1), 37-59.

Astley, R. and Coyette, J.P. (2001), "The performance of spheroidal infinite elements", *Int. J. Numer. Method. Eng.*, **52**(12), 1379-1396.

Astley, R. and Hamilton, J. (2006), "The stability of infinite element schemes for transient wave problems", *Comput. Method. Appl. Mech. Eng.*, **195**(29), 3553-3571.

Bao, Y., Ye, G., Ye, B. and Zhang, F. (2012), "Seismic evaluation of soil-foundation-superstructure system considering geometry and material nonlinearities of both soils and structures", *Soil. Found.*, **52**(2), 257-278.

Behnamfar, F. and Banizadeh, M. (2016), "Effects of soil-structure interaction on distribution of seismic vulnerability in RC structures", *Soil Dyn. Earthq. Eng.*, **80**, 73-86.

Bettess, P. (1992), *Infinite elements*, Penshaw Press.

Chopra, A.K. and Gutierrez, J.A. (1974), "Earthquake response analysis of multistorey buildings including foundation interaction", *Earthq. Eng. Struct. Dyn.*, **3**(1), 65-77.

Deng, L. and Kutter, B.L. (2012), "Characterization of rocking shallow foundations using centrifuge model tests", *Earthq. Eng. Struct. Dyn.*, **41**(5), 1043-1060.

Duggal, S. (2000), *Design of steel structures*, Tata McGraw-Hill Education.

Elgamal, A., Yan, L., Yang, Z. and Conte, J.P. (2008), "Three-dimensional seismic response of Humboldt Bay bridge-foundation-ground system", *J. Struct. Eng.*, **134**(7), 1165-1176.

Feldgun, V., Karinski, Y., Yankelevsky, D. and Kochetkov, A. (2016), "A new analytical approach to reconstruct the acceleration time history at the bedrock base from the free surface signal records", *Soil Dyn. Earthq. Eng.*, **85**, 19-30.

Ghandil, M. and Behnamfar, F. (2015), "The near-field method for dynamic analysis of structures on soft soils including inelastic soil–structure interaction", *Soil Dyn. Earthq. Eng.*, **75**, 1-17.

Han, Y. (2002), "Seismic response of tall building considering soil-pile-structure interaction", *Earthq. Eng. Eng. Vib.*, **1**(1), 57-64.

Hibbitt, K. (2013), *ABAQUS: User's Manual*, Version 6.13, Hibbitt. Karlsson & Sorensen, Incorporated.

Hokmabadi, A.S., Fatahi, B. and Samali, B. (2014), "Physical modeling of seismic soil-pile-structure interaction for buildings on soft soils", *Int. J. Geomech.*, **15**(2), 04014046.

Huang, S., Ozcelik, O. and Gu, Q. (2015), "A practical and efficient coupling method for large scale soil-structure interaction problems", *Soil Dyn. Earthq. Eng.*, **76**, 44-57.

Isbiliroglu, Y., Taborda, R. and Bielak, J. (2014), "Multiple structure-soil-structure interaction and coupling effects in building clusters", *Tenth U.S. National Conference on Earthquake Engineering Frontiers of Earthquake Engineering*, 10NCEE Anchorage, Alaska, July.

Koutsourelakis, S., Prévost, J.H. and Deodatis, G. (2002), "Risk assessment of an interacting structure-soil system due to liquefaction", *Earthq. Eng. Struct. Dyn.*, **31**(4), 851-879.

Krishnamoorthy, A. and Anita, S. (2016), "Soil-structure interaction analysis of a FPS-isolated structure using finite element model", Paper presented at the Structures.

Liu, W., Hutchinson, T.C., Kutter, B.L., Hakhamaneshi, M., Aschheim, M.A. and Kunnath, S.K. (2012), "Demonstration of compatible yielding between soil-foundation and superstructure components", *J. Struct. Eng.*, **139**(8), 1408-1420.

Lou, M., Wang, H., Chen, X. and Zhai, Y. (2011), "Structure-soil-structure interaction: literature review", *Soil Dyn. Earthq. Eng.*, **31**(12), 1724-1731.

Manolis, G.D. and Markou, A. (2012), "A distributed mass structural system for soil-structure-interaction and base isolation studies", *Arch. Appl. Mech.*, **82**(10-11), 1513-1529.

Matinmanesh, H. and Asheghabadi, M.S. (2011), "Seismic analysis on soil-structure interaction of buildings over sandy soil", *Procedia Eng.*, **14**, 1737-1743.

Merritt, F.S. (1996), "Minimum design loads for buildings and other structures: American society of civil engineers standard 7-95", *J. Architec. Eng.*, **2**(2), 80-81.

Mohasseb, S. and Abdollahi, B. (2009), "Soil-structure interaction analyses using cone models", *J. Seismol. Earthq. Eng.*, **10**(4), 167.

Rayhani, M. and El Naggar, M.H. (2008), "Numerical modeling of seismic response of rigid foundation on soft soil", *Int. J. Geomech.*, **8**(6), 336-346.

Reyes, J.C. and Kalkan, E. (2011), "Required number of records for ASCE/SEI 7 ground motion scaling procedure", *US Geological Survey Open-File Report*, **1083**(2011), 34.

Sharma, E.P., Ankit, E. and Singh, E.I.P. (2014), "Soil structure interaction effect on an asymmetrical RC building with shear walls", *IOSR J. Mech. Civ. Eng. (IOSR-JMCE)*, **11**(3), 45-56.

Trombetta, N., Mason, H., Chen, Z., Hutchinson, T., Bray, J. and Kutter, B. (2013), "Nonlinear dynamic foundation and frame structure response observed in geotechnical centrifuge experiments", *Soil Dyn. Earthq. Eng.*, **50**, 117-133.

Wolf, J.P. (1985), "Dynamic soil-structure interaction", Prentice Hall int.

Wolf, J.P. and Deeks, A.J. (2004), "Foundation vibration analysis: A strength of materials approach", Butterworth-Heinemann.

Yeganeh, N., Bazaz, J.B. and Akhtarpour, A. (2015), "Seismic analysis of the soil-structure interaction for a high rise building adjacent to deep excavation", *Soil Dyn. Earthq. Eng.*, **79**, 149-170.

Zhang, Y., Yang, Z., Bielak, J., Conte, J. and Elgamal, A. (2003), "Treatment of seismic input and boundary conditions in nonlinear seismic analysis of a bridge ground system", *Paper presented at the 16th ASCE Engineering Mechanics Conference*, University of Washington, Seattle, USA.

Zienkiewicz, O., Emson, C. and Bettess, P. (1983), "A novel boundary infinite element", *Int. J. Numer. Method. Eng.*, **19**(3), 393-404.

CC